The Transient Behaviour of a Differentially Heated Cavity with Isoflux Boundaries

S. Jiracheewanun[1], S. W. Armfield[1], M. Behnia[2] and G. D. McBain[1]
[1]School of Aerospace, Mechanical and Mechatronic Engineering,
University of Sydney, NSW, 2006 Australia
[2]Dean of Graduate Studies, University of Sydney, NSW, 2006 Australia

Abstract

In this study we investigate, using direct numerical simulation, the transient two-dimensional natural convection flow in a square cavity with isoflux side walls and adiabatic top and bottom boundaries. The equations of motion were solved using a non-iterative fractional-step pressure correction method which provides second-order accuracy in both time and space. Several features of the flow are identified and discussed in detail, in particular, the flow behaviour in the vertical thermal boundary layers along the side walls and in the horizontal intrusions adjacent to the top and the bottom boundaries. The results show that the transient flow features obtained for the isoflux cavity are similar to the flow features for the isothermal case. However, the fully developed flow features of the isoflux cavity are very different from the isothermal case.

Introduction

Natural convection in closed cavities has received a lot of attention because of its wide range of engineering applications. In the past, natural convection in a rectangular enclosure with vertical isothermal walls has been studied extensively, both experimentally and numerically. A classification of the development of the flow by Patterson & Imberger [1], a series of experiments by Ivey [2], and a comparison of numerical and experimental results by Patterson & Armfield [3] and Armfield & Patterson [4,5] are examples of previous isothermal cavity investigations. On the other hand, the cavity with isoflux walls has received much less attention. Kimura & Bejan [6] examined this case, but details of the flow features were not reported. The objectives of this study are to investigate the flow features from initiation until full development and compare the results with the isothermal cavity results of Patterson & Armfield [3].

Numerical Method
Governing Equations

The square cavity configuration is given in figure 1. The cavity is of width L, a uniform heat flux is specified along the no-slip side walls with isoflux in on the left wall and isoflux out on the right wall. The horizontal walls are adiabatic and no-slip. The governing equations are the two-dimensional Navier-Stokes and energy equations based on the Boussinesq assumption. The equations are written in non-dimensional form as follows:

$$\frac{\partial u}{\partial x} + \frac{\partial v}{\partial y} = 0 \tag{1}$$

$$\frac{\partial u}{\partial t} + u\frac{\partial u}{\partial x} + v\frac{\partial u}{\partial y} = -\frac{\partial p}{\partial x} + \left(\frac{\partial^2 u}{\partial x^2} + \frac{\partial^2 u}{\partial y^2}\right) \tag{2}$$

$$\frac{\partial v}{\partial t} + u\frac{\partial v}{\partial x} + v\frac{\partial v}{\partial y} = -\frac{\partial p}{\partial y} + \left(\frac{\partial^2 v}{\partial x^2} + \frac{\partial^2 v}{\partial y^2}\right) + \frac{Ra}{Pr}T \tag{3}$$

$$\frac{\partial T}{\partial t} + u\frac{\partial T}{\partial x} + v\frac{\partial T}{\partial y} = \frac{1}{Pr}\left(\frac{\partial^2 T}{\partial x^2} + \frac{\partial^2 T}{\partial y^2}\right) \tag{4}$$

where u and v are the velocity components in the x- and y-direction, t is time, p is pressure and T is temperature. In these equations, velocity is non-dimensionalized by $U=\upsilon/L$, length by

L, time by L^2/υ, pressure by $\rho(\upsilon/L)^2$, and $(T-T_o)$ by $q''L/k$. Prandtl number and Rayleigh number are defined as,

$$Pr = \frac{\upsilon}{\alpha}$$

$$Ra = \frac{g\beta q''L^4}{\alpha\upsilon k} \tag{5}$$

where β is the coefficient of volume expansion, q'' is heat flux, α is the thermal diffusivity, υ is the kinematic viscosity and k is the thermal conductivity.
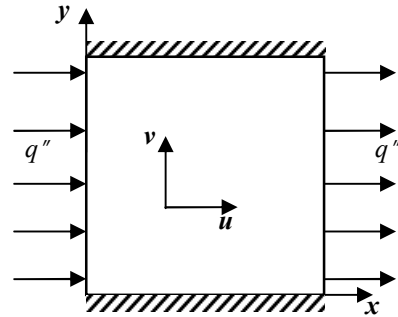

Figure. 1 Computational domain and coordinate system.

The corresponding dimensionless initial and boundary conditions are

$$T = u = v = 0 \quad \text{at all x, y and t<0}$$
$$T_x = -1 \qquad \text{on } x = 0,1$$
$$T_y = 0 \qquad \text{on } y = 0,1$$
$$u = v = 0 \qquad \text{on } x = 0,1 \text{ and } y = 0,1 \tag{6}$$

Discretization

Because of the large variation in length scales it is necessary to use a mesh that concentrates points in the boundary layer and is relatively coarse in the interior. The meshes are constructed using an exponentially stretched grid. The basic mesh uses 110x110 grid points, which are distributed symmetrically with respect to the domain half-width and half-height. The smallest grid size, near the boundaries, is 0.002. Away from the boundaries, the mesh stretching factor is 1.05. The mesh is generated with this expanding rate until it reaches half of the domain, resulting in a coarse mesh in the interior. The time step used was 1×10^{-5}.

The direct numerical simulations have been carried out using a finite volume method. The governing equations are discretized on a non-staggered mesh, with standard second-order central differencing used for the viscous, pressure gradient, and divergence terms, whereas the QUICK third-order upwind scheme is used for the advective terms. The momentum and temperature equations are solved using an ADI scheme. The second-order Adams-Bashforth scheme and Crank-Nicolson scheme are used for the time integration of the advective terms and the diffusive terms, respectively. To enforce continuity, the non-iterative fractional-step pressure correction method is used to construct a Poisson equation, which is solved using the Preconditioned Conjugate Gradient method.

Results

Results will be obtained with the isoflux boundary condition for $Ra=1x10^{10}$ and $Pr=7.5$, with the general flow structure and behaviour compared to those presented in Patterson & Armfield [3] for isothermal boundary conditions. The Patterson & Armfield [3] results were presented in dimensional form for a square cavity of height 0.24 m (h=0.24m) and obtained for Ra^*=3.26 $x10^8$ and Pr=7.5 where $Ra^*=g\beta\Delta Th^3/\upsilon\alpha$. A summary of the results obtained by Patterson & Armfield [3] is as follows.

Patterson & Armfield [3] divided the flow development into two stages; the first stage from 0 to 150 s and the second stage from 150 s to full development, at approximately 1500 s. The first stage is associated with the development of thermal boundary layers on the heated and cooled walls, which can be seen in figure 2, which shows the temperature in the boundary layer at y = 0.12 m and x = 0.002 m from the hot wall, plotted against time, with both numerical and experimental results shown.
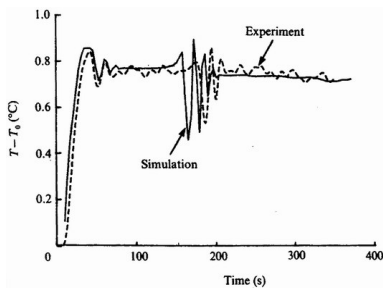

Figure. 2 Time traces of temperature at mid-height of the cavity for isothermal case with Ra^*=3.26x10^8 [3].

The initial rapid increase in temperature shows the thermal boundary layer growth, which at this height has reached full development by time 100 s. It is also observed that transition to full development in the boundary layer is associated with an oscillation in the signal, at approximately 40 s. This oscillation is caused by a series of waves travelling up the heated boundary layer, generated by the impulsive start-up of the system. The thermal boundary layers eject heated and cooled intrusions at the top and bottom of the hot and cold walls respectively. These intrusions travel across the cavity, with the heated intrusion in contact with the upper boundary and the cooled intrusion in contact with the lower boundary, striking and interacting with the base of the far wall boundary layer. This interaction perturbs the boundary layer, producing a second set of travelling waves that transit the boundary layer in the flow direction, seen in the second set of oscillations in figure 2, at approximately 170 s. The boundary layers are only able to entrain part of the intrusion flow, with the remainder rebounding from the far wall and setting up a seiching motion in the cavity. The development of the flow from this stage is associated with considerable activity in the intrusions, which gradually fill the cavity with stratified fluid. As the flow approaches full development the intrusion activity gradually diminishes, with the steady state flow consisting of a fully stratified interior with a cavity scale circulation, as shown in figure 3, where the flow is shown with the hot wall on the left.
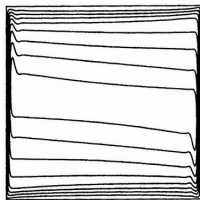

Figure 3. The mirror stream function contour in the isothermal cavity of Patterson & Armfield [3] at near steady state.

As noted above the isoflux boundary condition results presented here have been obtained with $Ra=1x10^{10}$. This value was chosen because it gave approximately the same thermal boundary layer thickness (3% of the cavity width) as the Ra^*=3.26x10^8 isothermal boundary condition case (compare figure 9(a), below, with figure 2(a) of Patterson & Armfield [3]). Figure 4 presents a temperature time series obtained at x= 0.01 and y = 0.5. Comparing this to figure 2 above, it is seen that the thermal boundary layer shows a qualitatively similar development, with an initial growth accompanied by a decaying oscillation followed by a second decaying oscillation. Both these sets of oscillations represent travelling waves, as in the isothermal case, with the initial set generated by the impulsive start-up and the second set generated by the intrusion striking the far wall. The general development for the isoflux boundary condition is therefore similar to that of the isothermal boundary condition.
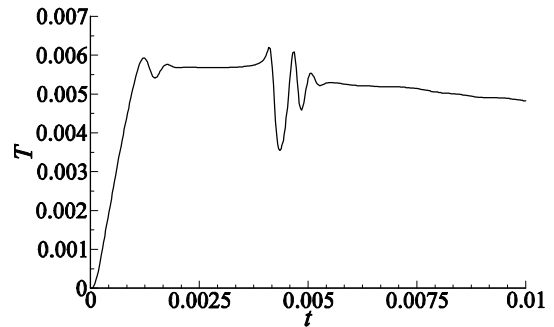

Figure. 4 Time traces of temperature at x=0.01, y=0.5 cavity for isoflux case with Ra=1.0x10^{10}.

Detailed flow development for the isoflux boundary condition is shown in figure 5, in the form of streamfunction contours. Figures 5(a-f) show 12 equally spaced contours between the maximum and minimum values, while figures 5(g-i) show 30 equally spaced contours, with the latter contour value chosen to more clearly demonstrate the features of the latter part of the development. In all cases the heated wall is on the left.
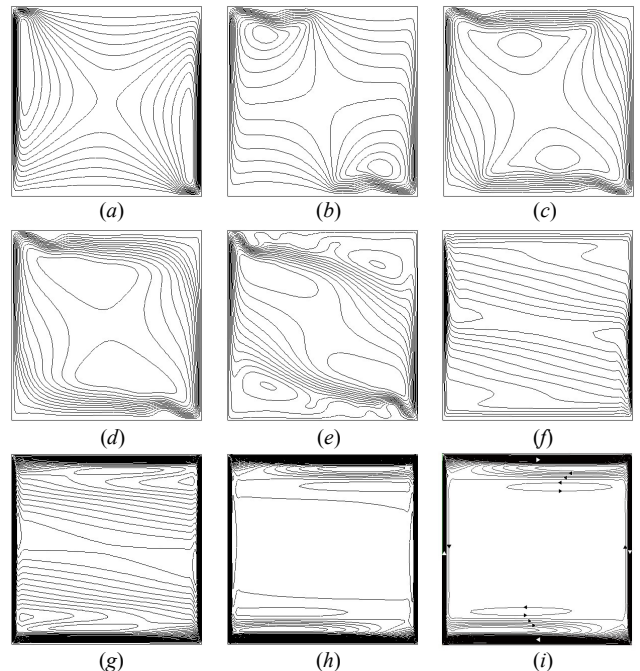

Figure. 5 Time evolution of the contours of stream function fields in the domain for Ra=1x10^{10}, Pr=7.5 at various times. (a) t=0.001; (b) t=0.002; (c) t=0.003; (d) t=0.004; (e) t=0.006; (f) t=0.025; (g) t=0.1; (h) t=0.55; (i) t=2.5.

For the isoflux boundary condition the flow development is most appropriately divided into three stages. The first stage, figures 5(a-c), is associated with the development of the thermal boundary layers, the generation of the intrusions, which are clearly seen travelling from the top of the heated wall towards the cooled wall, and vice-versa for the cooled wall, and the establishment of two circulations. The second stage, shown in figures 5(d-f), shows the intrusion striking the far walls, the generation of a separated backward flowing region within intrusions, and finally a cavity scale flow. The third stage, shown in figures 5(g-i), shows the full development of the flow in which the interior circulation gradually decays until finally the interior is quiescent, with flow only in the regions of the boundaries. This fully developed flow is complex, with an outer clockwise circulation following the boundary and an inner reverse circulation, as may be seen by the flow direction arrows included in figure 5(i). This reverse flow is accompanied by closed circulations adjacent to the horizontal boundaries, with additional interior reverse circulations also seen. However away from the horizontal boundaries the flow adjacent to the vertical boundaries is parallel to the boundaries. Temperature contours, presented in figure 6, show that at full development the cavity is fully stratified. The structure of the boundary layer adjacent to the vertical wall is seen in figure 7, which shows a horizontal profile of the vertical velocity at y=0.5. The inner region of reversing flow is clearly visible in the region x=0.027-0.055.
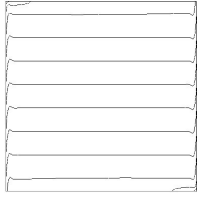

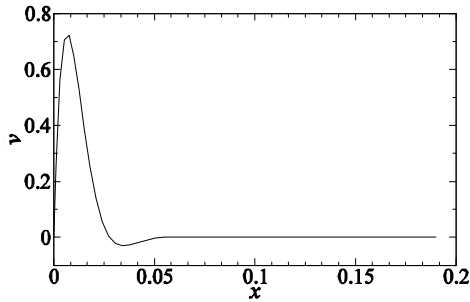Figure. 6 Temperature contour of fully developed flow t=2.5.

Figure. 7 Profile of vertical velocity along horizontal distance from the hot wall at y=0.5.

The first two stages of flow for the isoflux boundary condition are very similar to the isothermal boundary condition, with similar boundary and intrusion growth, two sets of travelling boundary layer waves with the same generation mechanisms, unsteady intrusion activity and eddy formation. The third stage however is quite different, indicating different heat transfer characteristics and scaling. It is therefore of interest to determine appropriate scalings for the isoflux boundary condition flow and compare them to scalings for the isothermal boundary condition flow. Scalings for the isoflux boundary condition flow may be obtained as follows. Combining the one-dimensional solution of Lietzke [7] with an energy balance relation [6] allows scalings to be obtained for the length, velocity and temperature for an evenly heated cavity of the following form;

$$\delta : 2^{5/9} Ra^{-2/9} \qquad (7)$$

$$U : 2^{5/3} Ra^{1/3} Pr^{-1} \qquad (8)$$

$$\Delta T : 2^{14/9} Ra^{-2/9} \qquad (9)$$

It is expected that these scalings will apply to the boundary layers on the cavity walls far enough away from the floor and ceiling such that the flow is approximately parallel. As observed above at Ra=1x10^{10} parallel regions of flow are observed adjacent to the walls and these scalings will therefore be tested for the boundary layer profiles obtained at the wall height.

Figure 8 contains the profiles of the vertical velocity at four Rayleigh numbers at steady state at y=0.5, with the raw data shown in figure 8(a). The profiles show the typical structure of the natural convection boundary layer. The scaling obtained indicates that velocity will scale with the 1/3 power of the Rayleigh number, while the boundary layer thickness will scale with the -2/9 power of the Rayleigh number. Scaled results are shown in figure 8(b). As can be seen the scaling brings all results onto a single curve indicating that the numerical velocity solution obeys the scaling relations.
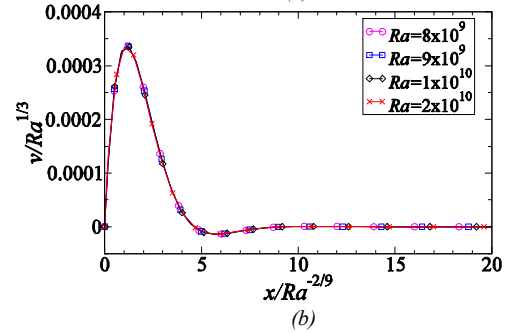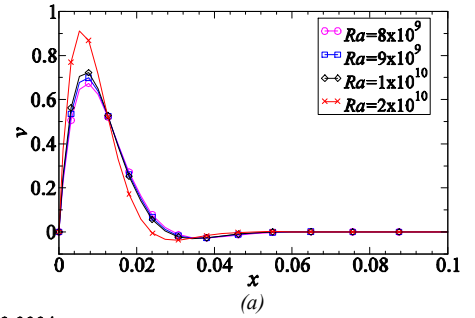

Figure. 8 Vertical velocity profiles of fully developed flow at various Ra; (a) raw data, (b) scaled data.
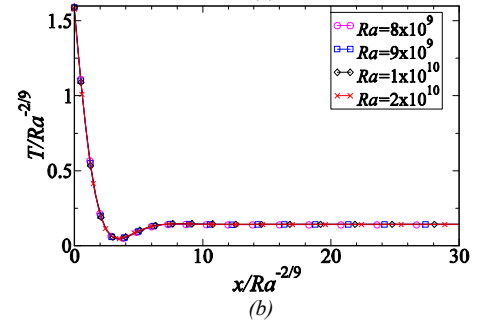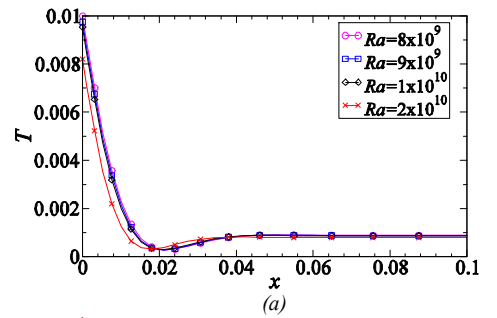

Figure. 9 Temperature profiles of fully developed flow at various Ra; (a) raw data, (b) scaled data.

The temperature profiles near the hot wall at steady state of four Rayleigh numbers at $y=0.5$ is shown in figure 9(a). The scaling obtained indicates that temperature will scale with the -2/9 power of the Rayleigh number, while the boundary layer thickness, again, will scale with the -2/9 power of the Rayleigh number as shown in figure 9(b). Again the scaling is seen to bring all the temperature profiles onto a single curve, validating the scaling relations.

The scaling results of the length and velocity for the natural convection in the cavity with isoflux boundaries at steady state can compared with the isothermal boundaries scalings of Patterson & Imberger [1] as summarized in table 1. It shows that the scaling results of the isoflux case differ from of the isothermal case [1] in every case. Thus, the Ra chosen for the present study is larger than Ra^{*} used for isothermal case [3] to yield approximately the same boundary layer thickness and development time as the isothermal case [3].

	Types of boundary	
	Isothermal [1]	Isoflux
Length scale	$x \sim Ra^{*\,-1/4}$	$x \sim Ra^{-2/9}$
Velocity scale	$v \sim Ra^{*\,1/2}$	$v \sim Ra^{1/3} Pr^{-1}$

Table 1. The comparison of length and velocity scaling results of the isothermal case [1] and of the isoflux case.

Conclusion

The flow features in the first two stages of flow development, described above, are similar to those for the isothermal boundary condition case, described by Patterson & Armfield [3]. However the fully developed flow is quite different with the isoflux boundary condition cavity having a flow only in the vicinity of the boundaries, with a quiescent core. The isothermal boundary condition cavity displays cavity scale circulation with a non-quiescent core. Clearly the interaction of the isoflux boundary condition with the cavity flow is different to that of the isothermal boundary condition. The scalings for the fully developed isoflux boundary condition flow have also been found to be different to those of the isothermal boundary condition flow. The length scale for the isoflux case will be reduced more rapidly with increasing Rayleigh number, while the velocity scale will be increased more rapidly.

References

[1] Patterson, J. and Imberger, J., Unsteady natural convection in a rectangular cavity, *J. Fluid Mech.,* **100**, 1980, 65-86.

[2] Ivey, G. N., Experiments on transient natural convection in a cavity, *J. Fluid Mech.,* **144**, 1984 , 389-401.

[3] Patterson, J.C. and Armfield, S.W., Transient features of natural convection in a cavity, *J. Fluid Mech.*, **219**, 1990, 469-497.

[4] Armfield, S.W. and Patterson, J.C., Direct simulation of wave interactions in unsteady convection in a cavity, *Int. J. Heat Mass Transfer*, **34**, 1991, 929-940.

[5] Armfield, S.W. and Patterson, J.C., Wave properties of natural-convection boundary layers, *J. Fluid Mech.*, **239**, 1992, 195-211.

[6] Kimura, S. and Bejan, A., The boundary layer natural convection regime in a rectangular cavity with uniform heat flux from the side, *J. Heat Transfer*, **106**, 1984, 98-105.

[7] Lietzke, A. F., Theoretical and experimental investigation of heat transfer by laminar natural convection between parallel plates, Report 1223, NACA, 1955.